Octupolar order in *d*-orbital Mott insulators

A. Paramekanti,[1,2,*] D. D. Maharaj ⓘ,[3] and B. D. Gaulin[3,4,5]

[1]*Department of Physics, University of Toronto, 60 St. George Street, Toronto, Ontario, Canada M5S 1A7*
[2]*International Centre for Theoretical Sciences, Tata Institute of Fundamental Research, Bengaluru 560089, India*
[3]*Department of Physics and Astronomy, McMaster University, Hamilton, Ontario, Canada L8S 4M1*
[4]*Brockhouse Institute for Materials Research, McMaster University, Hamilton, Ontario, Canada L8S 4M1*
[5]*Canadian Institute for Advanced Research, 661 University Ave., Toronto, Ontario, Canada M5G 1M1*

Motivated by experimental and theoretical interest in realizing multipolar orders in *d*-orbital materials, we discuss the quantum magnetism of $J = 2$ ions which can be realized in spin-orbit coupled oxides with $5d^2$ transition metal ions. Based on the crystal-field environment, we argue for a splitting of the $J = 2$ multiplet, leading to a low-lying non-Kramers doublet which hosts quadrupolar and octupolar moments. We discuss a microscopic mechanism whereby the combined perturbative effects of orbital repulsion and antiferromagnetic Heisenberg spin interactions leads to ferro-octupolar coupling between neighboring sites, and stabilizes ferro-octupolar order for a face-centered cubic lattice. This same mechanism is also shown to disfavor quadrupolar ordering. We show that studying crystal field levels via Raman scattering in a magnetic field provides a probe of octupolar order. We study spin dynamics in the ferro-octupolar state using a slave-boson approach, uncovering a gapped and dispersive magnetic exciton. For sufficiently strong magnetic exchange, the dispersive exciton can condense, leading to conventional type-I antiferromagnetic (AFM) order which can preempt octupolar order. Our proposal for ferrooctupolar order, with specific results in the context of a model Hamiltonian, provides a comprehensive understanding of thermodynamics, μSR, x-ray diffraction, and inelastic neutron-scattering measurements on a range of cubic $5d^2$ double perovskite materials including Ba_2ZnOsO_6, Ba_2CaOsO_6, and Ba_2MgOsO_6. Our proposal for exciton condensation leading to type-I AFM order may be relevant to materials such as Sr_2MgOsO_6.

I. INTRODUCTION

Multipolar symmetry-breaking orders have been extensively discussed in *f*-orbital-based lanthanide and actinide compounds, which host ions where spin-orbit coupling (SOC) is a dominant energy scale [1]. For instance, the "hidden order" state of URu_2Si_2 has been extensively investigated as potentially arising from complex multipolar symmetry breaking [2–4]. Another well-known example is cubic NpO_2 [5–8], where a large body of experiments have been reconciled in terms of a primary antiferro-triakontadipolar rank-five magnetic multipolar) symmetry breaking which drives secondary antiferro-quadrupolar order. In certain pyrochlore magnets, all-in all-out magnetic order has been proposed to lead to "effective octupoles" on tetrahedra [9]. Ongoing experimental [10–12] and theoretical investigations [13–16] of $PrTi_2Al_{20}$ and PrV_2Al_{20} have also uncovered quadrupolar and ferro-octupolar orders.

Recently, unconventional multipolar orders have also been proposed in *d*-orbital metals to occur as Pomeranchuk instabilities of spin-orbit-coupled Fermi surfaces [17]. Specifically, metallic oxides which have *d*-orbital ions with large SOC, such as $LiOsO_3$ and $Cd_2Re_2O_7$, have been proposed as potential candidates to realize this physics [17]. Experiments have indeed discovered an odd-parity nematic metal in $Cd_2Re_2O_7$ below $T_c \sim 200$ K via optical second-harmonic generation [18]. Other proposed materials for hosting multipolar orders include A_2OsO_4 (with $A = $ K, Rb, Cs) [19]. However, to the best of our knowledge, there have been no clear *d*-orbital candidates for hosting octupolar orders. Indeed, there appears to be no microscopic understanding of what the key ingredients are to potentially stabilize such octupolar phases.

In this paper, we consider spin-orbit-coupled Mott insulators having transition-metal ions with total angular momentum $J = 2$. We show that such Mott insulators can exhibit competing multipolar orders and discuss a microscopic mechanism which stabilizes a ferro-octupolar state on the face-centered cubic (FCC) lattice. We show how nonresonant Raman scattering may probe the octupolar order and compute the dynamic spin structure factor which can be measured using neutron-scattering experiments. Our work in this paper is directly motivated by a series of recent experiments on cubic double perovskite (DP) magnets and we discuss how our results apply to these materials.

II. BACKGROUND REVIEW

Ordered DP materials, with chemical formula $A_2BB'O_6$, are of great interest in the context of frustrated magnetism since the B and B′ sublattices individually form networks of edge-sharing tetrahedra. When only one of these ions (say, B′) is magnetically active, it results in quantum magnetism on

*arunp@physics.utoronto.ca

054439-1

the FCC lattice, a prototypical setting for exploring geometric frustration in Mott insulators. Such DP Mott insulators have been studied for various electronic fillings d^1-d^5, and we briefly review some key results below.

For d-orbitals in an octahedral crystal field, the t_{2g} single-particle levels associated with the magnetic B' ion are split by SOC, resulting in a fourfold degenerate, $j_{\text{eff}} = 3/2$, ground state and a doubly degenerate, $j_{\text{eff}} = 1/2$, excited state. The physics of such materials then depends strongly on the electronic filling, d^1-d^5, of these t_{2g} states. For the most well-studied d^5 electronic configuration (e.g., for Ir^{4+} or Ru^{3+} ions), this results in a single hole in a $j_{\text{eff}} = 1/2$ state [20,21]. Recent experimental and theoretical studies on the DP Ba_2CeIrO_6, which hosts such a $j_{\text{eff}} = 1/2$ Mott insulator on the FCC lattice, have found evidence of magnetic ordering with a strong frustration parameter, suggesting proximity to a quantum spin-liquid state [22,23]. Stepping down to a d^4 configuration, strong SOC favors a total $J_{\text{eff}} = 0$ singlet ground state, with a gap to all excitations [24], which appears to be realized in Ba_2YIrO_6 [25–28]. However, if intersite exchange competes with SOC, it can lead to magnetic ordering from exciton condensation [24,29]; clear experimental candidates for such an exciton condensate are yet to be found. Further down, a d^3 configuration would naively be expected to form an orbital singlet state with spin $S = 3/2$; however, neutron scattering and resonant inelastic x-ray scattering experiments have found that $5d$ transition metal oxides belly this expectation, finding magnetically ordered states with large spin gaps which clearly reveal the dominance of SOC over Hund's coupling [30–32]. Skipping to d^1 ions, we are led to a $j_{\text{eff}} = 3/2$ angular momentum state. Theoretical studies of such moments on the FCC lattice have shown that incorporating important intersite orbital repulsion can lead to complex multipolar exchange interactions, stabilizing wide regimes of quadrupolar order in the phase diagram [33–35] which may coexist with conventional dipolar magnetic order, or valence bond orders [36]. Indeed, recent experiments on $5d^1$ oxides, Ba_2NaOsO_6 with Os^{7+} [37,38] and Ba_2MgReO_6 with Re^{6+} [39], have found clear evidence for multiple transitions associated with these distinct broken symmetries, with a higher temperature quadrupolar ordering transition followed by dipolar ordering at a lower temperature.

Finally, we turn to the topic of our work: d^2 ions with an effective $J_{\text{eff}} = 2$ angular momentum state. In this case, previous theoretical work has found intricate multipolar couplings as for d^1 filling and broad swaths of quadrupolar orders in the phase diagram [33–35]. In this paper, in contrast to previous work, we make the case that $J_{\text{eff}} = 2$ quantum magnets in a cubic environment may instead support ground states with ferro-octupolar order. We show that this can lead to a consistent understanding of a large body of experimental data on the family of cubic DP materials Ba_2MOsO_6 (with $M = Zn$, Mg, Ca), including specific heat, magnetic susceptibility, x-ray diffraction, powder neutron diffraction, muon spin relaxation (μSR), and inelastic neutron scattering. We present a microscopic mechanism which leads to ferro-octupolar coupling, make predictions for how Raman scattering might uncover octupolar order, and compute the dynamic spin structure factor which shows a gapped magnetic exciton. Our results

point to Ba_2MOsO_6 DPs as rare examples of octupolar order in d-orbital systems.

III. EFFECTIVE LOCAL MODEL

We start from an effective $J = 2$ local moment, as appropriate for d^2 ions arising from coupling total $L = 1$ and $S = 1$ for two electrons. The most general form of the octahedral crystal field Hamiltonian for $J = 2$ ions is given by [40]

$$H_{\text{CEF}} = -V_{\text{eff}}(\mathcal{O}_{40} + 5\mathcal{O}_{44}). \quad (1)$$

Here, the Steven's operators are given by

$$\mathcal{O}_{40} = 35J_z^4 - (30J(J+1) - 25)J_z^2 + 3J^2(J+1)^2 \\ - 6J(J+1), \quad (2)$$

$$\mathcal{O}_{44} = \tfrac{1}{2}(J_+^4 + J_-^4). \quad (3)$$

For $V_{\text{eff}} > 0$, this results in a non-Kramers ground-state doublet and an excited triplet with a gap $\Delta = 120V_{\text{eff}}$. As shown in a parallel publication [40], working in the $|J_z = m\rangle$ basis leads to ground-state wave functions,

$$|\psi_{g,\uparrow}\rangle = |0\rangle, \quad |\psi_{g,\downarrow}\rangle = \frac{1}{\sqrt{2}}(|2\rangle + |-2\rangle), \quad (4)$$

and excited state wave functions,

$$|\psi_{e,\pm}\rangle = |\pm 1\rangle; \quad |\psi_{e,0}\rangle = \frac{1}{\sqrt{2}}(|2\rangle - |-2\rangle). \quad (5)$$

The ground-state manifold has vanishing matrix elements for the dipole operators (J^z, $J^\pm$), precluding any dipolar order stemming from the low-energy doublet manifold. However, $\vec{J}$ can induce transitions between the ground doublet and the excited triplet, which will lead to a spin-gap Δ in the excitation spectrum. As discussed below, incorporating intersite AFM exchange would convert this local mode into a dispersing gapped "magnetic exciton."

We have previously shown (see Supplemental Material of Ref. [40]) that this simple model can reasonably account for the measured entropy and magnetic susceptibility in the $5d^2$ DP Mott insulators Ba_2MOsO_6 (with $M = Zn$, Mg, Ca). Defining pseudospin-1/2 operators $\vec{\tau}$ within the ground-state doublet, we find that the e_g quadrupolar operators ($J_x^2 - J_y^2) \equiv 2\sqrt{3}\tau_x$, $(3J_z^2 - J^2) \equiv -6\tau_z$, while the octupolar operator $\overline{J_xJ_yJ_z} \equiv -\sqrt{3}\tau_y$ (where overline denotes symmetrization). Thus, the ground doublet can lead to time-reversal invariant quadrupolar symmetry breaking from ordering in the (τ_x, τ_z) plane, which would also cause noncubic distortions due to accompanying orbital order. Alternatively, octupolar ordering with $\langle\tau_y\rangle \neq 0$ will lead to spontaneously broken time-reversal symmetry without noncubic distortions. Finally, if the gapped magnetic exciton is sufficiently dispersive, with a bandwidth larger than the spin gap, it can Bose condense and lead to dipolar magnetic order.

IV. ORIGIN OF FERROOCTUPOLAR COUPLING

We next consider projecting microscopic intersite interactions into the low-energy doublet sector described by the

pseudospin-1/2 operators $\vec{\tau}$. We have two types of interactions to consider here: type-I couplings have nonzero weight in the doublet sector can be directly projected into this subspace, while type-II operators which mix the doublet and triplet sectors will contribute within perturbation theory.

Examples of type-I interactions may be illustrated by considering a pair of neighboring sites in the xy plane which will have interactions between the e_g quadrupolar charge densities $(J_x^2 - J_y^2)$ or $(3J_z^2 - J^2)$ at the two sites. These interactions may be directly projected into the doublet sector as

$$H_{\text{eff},xy}^{(1)} = \sum_{\langle ij \rangle_{xy}} (-\gamma_0 \tau_{ix}\tau_{jx} + \gamma_1 \tau_{iz}\tau_{jz}), \tag{6}$$

with $\gamma_0, \gamma_1 > 0$. (The effective Hamiltonian for nearest neighbors in other planes can be obtained using symmetry transformations.)

Examples of type-II interactions for a pair of neighboring spins in the xy plane include the conventional AFM exchange $\gamma_m \vec{J}_i \cdot \vec{J}_j$ with $\gamma_m > 0$, where $\vec{J}$ denotes the $J = 2$ spin. In addition, they include t_{2g} quadrupolar interactions of the form $\gamma_2 \rho_{i,xy}\rho_{j,xy}$, where $\rho_{i,xy} = (J_{ix}J_{iy} + J_{iy}J_{ix})/2$ and $\gamma_2 > 0$. In this case, neither $\vec{J}_i$ nor $\rho_{i,xy}$ have matrix elements in the low-energy doublet space $|L\rangle$, but they instead mix $|L\rangle$ into the high-energy triplet subspace $|H\rangle$, with an energy cost 2Δ since both sites (i, j) get excited into the triplet sector. We find that the effective Hamiltonian for such neighboring spins in the xy plane is given, in second-order perturbation theory, by

$$H_{\text{eff},xy}^{(2)} = -\frac{1}{2\Delta} \sum_{\langle ij \rangle_{xy}} (\gamma_m \vec{J}_i \cdot \vec{J}_j + \gamma_2 \rho_{i,xy}\rho_{j,xy})^2. \tag{7}$$

Projecting these operators to the doublet sector, we find

$$H_{\text{eff},xy}^{(2)} = -\frac{1}{2\Delta} \sum_{\langle ij \rangle_{xy}} \left[12\gamma_m\gamma_2 \tau_{iy}\tau_{jy} + \left(6\gamma_m^2 + \frac{9}{4}\gamma_2^2\right)\tau_{iz}\tau_{jz} \right.$$
$$\left. + \left(6\gamma_m^2 - 12\gamma_m\gamma_2\right)\tau_{ix}\tau_{jx} \right]. \tag{8}$$

This equation is one of the key results of our paper. The first term shows that the second-order perturbation theory produces a ferro-octupolar coupling with strength $6\gamma_m\gamma_2/\Delta$ from the cross-coupling of γ_2 and γ_m. Furthermore, assuming a hierarchy $\gamma_m \ll \gamma_2$, we see that the net quadrupolar interaction, after including the terms in Eq. (6), involves direct and perturbative contributions which come with opposite signs,

$$H_{xy}^{\text{Quad}} = \sum_{\langle ij \rangle_{xy}} \left[\left(-\gamma_0 + 6\frac{\gamma_m\gamma_2}{\Delta}\right)\tau_{ix}\tau_{jx} + \left(\gamma_1 - \frac{9}{8}\frac{\gamma_2^2}{\Delta}\right)\tau_{iz}\tau_{jz} \right]. \tag{9}$$

This partial cancellation of quadrupolar couplings may cause suppression of quadrupolar order, allowing for the ferro-octupolar coupling to dominate. We thus identify the key microscopic mechanism underlying ferrooctupolar ordering. A complete theory starting from an electronic hopping model with interactions, along the lines of calculations presented in Refs. [19,33–35,41], is left for future work.

V. RAMAN SCATTERING AS A PROBE OF OCTUPOLAR ORDER

We next turn to magnetic Raman scattering [42] in such systems given its usefulness as a probe of crystal field levels and quadrupolar order in heavy fermion compounds [43]. We show that Raman scattering in a nonzero magnetic field strikingly leads to additional modes in the presence of octupolar order.

Our work builds on a recent study by Patri *et al.* [16], which revealed an unusual magnetoelastic coupling between the strain and the octupolar order induced by a magnetic field, which leads to linear-in-field magnetostriction as a hallmark of octupolar order. They argued that octupolar ordering may also lead to a softening of certain phonon modes in the presence of a magnetic field, which may be detectable by Raman scattering. Here, by contrast, we focus on the impact of octupolar ordering on the crystal-field levels themselves.

The nonresonant Raman scattering intensity is given by the expression [42]

$$\mathcal{I}_{\mu\nu}(\omega) = \sum_{i,f} \mathcal{P}_i |\langle f|R_{\mu\nu}|i\rangle|^2 \delta(E_f - E_i - \hbar\omega), \tag{10}$$

where i, f refer to initial and final states, with corresponding energies E_i, E_f, and $\mathcal{P}_i$ is the (thermal) occupation probability of the initial state. The Raman operator $R_{\mu\nu}$ depends on the polarizations $\hat{\varepsilon}$ of the incoming and outgoing photons which differ in frequency by $\hbar\omega$. Here, we will focus on the specific Raman operator corresponding to $\hat{\varepsilon}_{\text{in}} \parallel \hat{x}$ and $\hat{\varepsilon}_{\text{out}} \parallel \hat{y}$, which, on symmetry grounds, is given by $R_{xy} = (J_xJ_y + J_yJ_x)/2$.

To explore the crystal-field levels of the $J = 2$ ion in the presence of octupolar order and a nonzero magnetic field $B\hat{z}$, we modify the crystal-field Hamiltonian in Eq. (1) as

$$H_{\text{loc}} = H_{\text{CEF}} - \mathcal{B}_{\text{oct}} \sum_i \tau_{iy} - B \sum_i J_{i,z}, \tag{11}$$

where $\mathcal{B}_{\text{oct}}$ is the ferro-octupolar Weiss field in the symmetry broken phase. This Weiss field does not impact the excited triplet wave functions which cost energy Δ, but splits the non-Kramers doublet to form eigenstates

$$|\phi_\pm\rangle = \frac{1}{\sqrt{2}}(|\psi_{g,\uparrow}\rangle \pm i|\psi_{g,\downarrow}\rangle), \tag{12}$$

which have their energies shifted, respectively, by $\mp\mathcal{B}_{\text{oct}}$. We focus here on the zero temperature behavior of the Raman spectrum in this local limit.

For $B = 0$, it is easy to show that the Raman operator R_{xy} has no matrix elements in the low-energy sector $\{|\phi_\pm\rangle\}$. Instead, at zero temperature, it induces transitions between the octupolar ground state $|\phi_+\rangle$ and the excited crystal-field state $|\psi_{e,0}\rangle$ at energy $\Delta + \mathcal{B}_{\text{oct}}$. The main panel of Fig. 1 depicts this mode, which is obtained by diagonalizing H_{loc} and computing $\mathcal{I}_{xy}(\omega)$. Here, we have artificially introduced a broadening $\sim 0.02\Delta$ to mimic resolution effects.

Switching on $B \neq 0$ mixes the doublet and triplet wave functions at $\mathcal{O}(B/\Delta)$, so we must work with perturbed low-energy doublet eigenstates

$$|\phi_\pm'\rangle = |\phi_\pm\rangle \pm i\sqrt{2}\frac{B}{\Delta \pm \mathcal{B}_{\text{oct}}}|\psi_{e,0}\rangle. \tag{13}$$

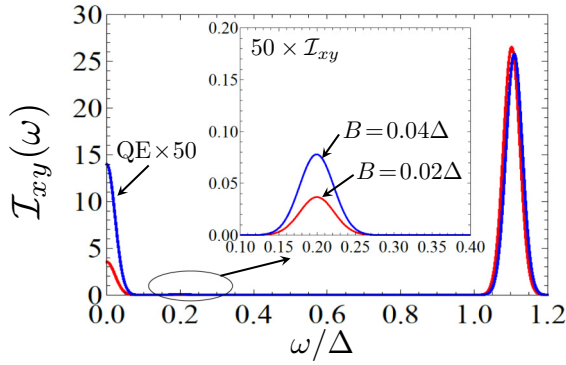FIG. 1. Main panel: Raman intensity $\mathcal{I}_{xy}(\omega)$ as a function of frequency ω in units of the doublet-triplet gap Δ, in the presence of an octupolar Weiss field $\mathcal{B}_{oct} = 0.1\Delta$, for magnetic field $B\hat{z}$ with $B = 0.02\Delta$ (red) and $B = 0.04\Delta$ (blue). The dominant peak is at $\omega = \Delta + \mathcal{B}_{oct}$, while QE refers to the B-induced quasielastic part in the presence of octupolar order, which we have scaled up by a factor of 50. Inset: Rescaled $\mathcal{I}_{xy}$ zoomed in at small low nonzero frequency, showing an additional mode emerging for $B \neq 0$ at a frequency $\omega \sim 2\mathcal{B}_{oct}$, corresponding to the transition between the two doublet states split by octupolar order.

In addition to a weak renormalization of the above crystal-field transition, this leads to two effects. First, we find that

$$\langle \phi'_+ | R_{xy} | \phi'_+ \rangle = -2\sqrt{3} \frac{B}{\Delta + \mathcal{B}_{oct}}, \quad (14)$$

which is closely tied to the linear-in-field magnetostriction explored by Patri *et al.* [16] and should lead to a quasielastic Raman signal with strength $|\langle \phi'_+ | R_{xy} | \phi'_+ \rangle|^2 \propto B^2/(\Delta + \mathcal{B}_{oct})^2$. Remarkably, a striking parallel of such a quasielastic field-induced mode was discussed long ago in the context of (resonant) B_{2g} Raman scattering to probe uniform scalar spin chirality in insulating square lattice antiferromagnets [44,45]. The spin chirality breaks time reversal but preserves spin-rotation symmetry, being similar, in this sense, to octupolar order.

In addition, we uncover a Raman mode corresponding to a $|\phi'_+\rangle \rightarrow |\phi'_-\rangle$ transition at an energy $\approx 2\mathcal{B}_{oct}$. For $B \ll \Delta - \mathcal{B}_{oct}$, the intensity of this mode scales $\propto B^2 \mathcal{B}_{oct}^2/(\Delta^2 - \mathcal{B}_{oct})^2$. The inset of Fig. 1 depicts this mode, which is obtained by diagonalizing H_{loc} and computing $\mathcal{I}_{xy}(\omega)$.

The quasielastic signal and the mode at $2\mathcal{B}_{oct}$ are un-ambiguous signatures of octupolar order. Both features lie well within the spin gap Δ. Temporally modulating B, or comparing the Raman intensity in a field relative to the zero field spectrum, might enable one to potentially search for these signals; however, their weak intensities render this a potentially challenging experiment.

VI. MAGNETIC EXCITONS AND DYNAMIC SPIN-STRUCTURE FACTOR

To explore, in more detail, the spin-excitation spectrum at energy scales on the order of the spin gap Δ, we use a slave boson approach [46–48]. The ensuing results can then be compared with existing inelastic neutron-scattering results

on Ba$_2M$OsO$_6$ [40]. We define the ground and excited states of the low-energy doublet via

$$|\psi_{g,\sigma}\rangle = b_\sigma^\dagger |\text{vac}\rangle, \quad (15)$$

$$|\psi_{e,\alpha}\rangle = d_\alpha^\dagger |\text{vac}\rangle, \quad (16)$$

where $\sigma = \uparrow, \downarrow$, $\alpha = 0, \pm$, and $|\text{vac}\rangle$ denotes the boson vacuum. This requires a local constraint:

$$\sum_{\sigma=\pm} b_\sigma^\dagger b_\sigma + \sum_{\alpha=0,\pm} d_\alpha^\dagger d_\alpha = 1. \quad (17)$$

Excitations out of the low-energy space contain at least one b boson; we thus get

$$J^+ = \sqrt{6}(b_\uparrow^\dagger d_- + d_+^\dagger b_\uparrow) + \sqrt{2}(b_\downarrow^\dagger d_+ + d_-^\dagger b_\downarrow), \quad (18)$$

$$J^z = 2(d_0^\dagger b_\downarrow + b_\downarrow^\dagger d_0). \quad (19)$$

Going beyond the simple local Hamiltonian, we model the dispersion of the gapped spin excitations using a nearest-neighbor Heisenberg exchange $\gamma_m \sum_{\langle ij \rangle} \vec{J}_i \cdot \vec{J}_j$. We supplement this, in the ferro-octupolar symmetry broken phase, by a uniform octupolar Weiss field: $-\mathcal{B}_{oct} \sum_i \tau_{iy}$. Here, $\tau_y \equiv -i(b_\uparrow^\dagger b_\downarrow - b_\downarrow^\dagger b_\uparrow)$, and, without loss of generality, we can set $\mathcal{B}_{oct} > 0$. The total Hamiltonian we study is thus

$$H_{spin} = H_{CEF} + \gamma_m \sum_{\langle ij \rangle} \vec{J}_i \cdot \vec{J}_j - \mathcal{B}_{oct} \sum_i \tau_{iy}. \quad (20)$$

The Weiss field favors a ground-state Bose condensate $b_\uparrow \approx 1/\sqrt{2}$ and $b_\downarrow \approx i/\sqrt{2}$, resulting in the simplified expressions

$$J^+ \approx \sqrt{3}(d_+^\dagger + d_-) - i(d_+ - d_-^\dagger), \quad (21)$$

$$J^z \approx i\sqrt{2}(d_0^\dagger - d_0). \quad (22)$$

Using these and accounting for the local doublet-triplet gap, we transform to momentum space, so the full Hamiltonian for describing the magnetic excitons is given by

$$H_{exc} = (\Delta + \mathcal{B}_{oct}) \sum_{\mathbf{k}\alpha} d_{\mathbf{k},\alpha}^\dagger d_{\mathbf{k},\alpha} + \frac{\gamma_m}{2} \sum_{\mathbf{k}} \eta_{\mathbf{k}} J_{\mathbf{k}}^+ J_{-\mathbf{k}}^-$$

$$- \gamma_m \sum_{\mathbf{k}} \eta_{\mathbf{k}} (d_{\mathbf{k},0}^\dagger - d_{-\mathbf{k},0})(d_{-\mathbf{k},0}^\dagger - d_{\mathbf{k},0}), \quad (23)$$

where $J_{\mathbf{k}}^+ \equiv \sqrt{3}(d_{\mathbf{k},+}^\dagger + d_{-\mathbf{k},-}) - i(d_{-\mathbf{k},+} - d_{\mathbf{k},-}^\dagger)$, $J_{-\mathbf{k}}^- \equiv (J_{\mathbf{k}}^+)^\dagger$, and $\eta_{\mathbf{k}} = \sum_\delta e^{i\mathbf{k}\cdot\delta}$ with δ labeling the 12 nearest-neighbor vectors on the FCC lattice. This leads to a threefold degenerate magnetic exciton with energy dispersion given by

$$\lambda(\mathbf{k}) = \sqrt{(\Delta + \mathcal{B}_{oct})(\Delta + \mathcal{B}_{oct} + 4\gamma_m \eta_{\mathbf{k}})}. \quad (24)$$

We find that the exciton energy $\lambda(\mathbf{k})$ is largest at the Γ point, and is softest at the typical FCC lattice type-I AF ordering wave vector $\mathbf{K}$.

We expect the exciton dispersion will have temperature dependence through the temperature dependence of the octupolar order parameter, which enters via the Weiss field $\mathcal{B}_o(T)$, softening somewhat as we heat up toward the octupolar order-ing transition. A plot of the dispersion along a high-symmetry path in the FCC Brillouin zone, for a choice $\mathcal{B}_{oct}/\Delta = 0.1$ and $\gamma_m/\Delta = 0.05$, is shown in Fig. 2. For sufficiently large
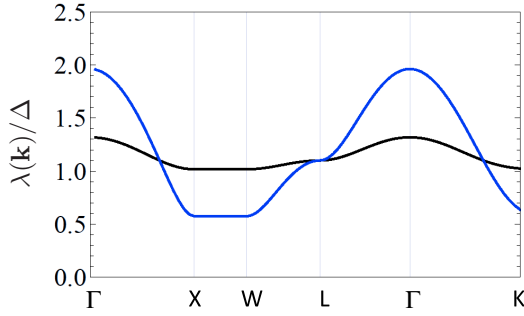
FIG. 2. Magnetic exciton dispersion $\lambda(\mathbf{k})$ (in units of Δ) along high-symmetry path in the FCC lattice Brillouin zone, for a choice of octupolar Weiss field $\mathcal{B}_{\text{oct}} = 0.1\Delta$ and two different choices for the Heisenberg coupling: (i) $\gamma_m = 0.01\Delta$ (black) and (ii) $\gamma_m = 0.05\Delta$ (blue). The exciton mode clearly softens with increasing γ_m.
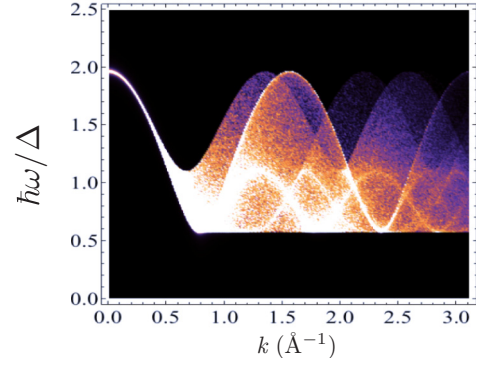

FIG. 3. Powder-averaged dynamic spin structure factor (arbitrary units) including the Os^{6+} form factor, showing the gapped magnetic exciton, as a function of momentum transfer k (in Å^{-1}, for a lattice constant $a = 4\,\text{Å}$) and energy $\hbar\omega$ (in units of Δ). We have set the Heisenberg exchange coupling $\gamma_m = 0.05\Delta$ and octupolar Weiss field $\mathcal{B}_o = 0.1\Delta$.

exchange coupling γ_m, the magnetic exciton can potentially condense, leading to coexistence of dipolar and octupolar orders. The dipolar order can even preempt octupolar order if $\gamma_m > \Delta/16$, leading to conventional type-I AFM order.

VII. EXPERIMENTAL IMPLICATIONS

The cubic osmates Ba_2MOsO_6 (with M = Zn, Mg, Ca) potentially provide a realization of $J = 2$ ions on the FCC lattice. They all exhibit a single phase transition at $T^* \sim 30$-50 K, across which the entropy release is only $\sim \ln(2)$ per Os, suggesting that the full $\ln(5)$ entropy is partially quenched for $T \lesssim 100$ K [49–51] without any phase transition. Indeed, the structure appears to be perfectly cubic, in the $Fm\bar{3}m$ space group, at all temperatures; both neutron diffraction and high resolution XRD measurements find no signs of any noncubic distortions [40]. This suggests that the entropy quenching above the phase transition at T^* must arise from symmetry-allowed crystal field effects, as discussed in our theory with a non-Kramers ground-state doublet.

Below the phase transition at T^*, neutron diffraction sees no ordered moment, even for $T \ll T^*$, instead placing tight upper bounds on the ordered dipolar moment, $\lesssim 0.06$–$0.13\mu_B$, depending on the material [40]. At the same time, μSR measurements have found evidence for zero-field oscillations, showing spontaneous breaking of time-reversal symmetry [49]. Since neutron diffraction strongly hints at the absence of dipolar magnetic order, and the cubic structure appears inconsistent with quadrupolar order, we argue that octupolar ordering within the doublet, which preserves cubic crystal symmetry and breaks time-reversal symmetry, provides the simplest explanation for the data. (Unlike for the Γ_5 multipoles in NpO_2 [1], which undergo triple-$\mathbf{Q}$ ordering, the ferro-octupolar ordering here is not symmetry constrained to induce secondary quadrupolar order.)

Inelastic neutron-scattering experiments [40] find a spin gap ~ 10–15 meV, which we interpret as arising from the doublet-triplet gap of the crystal-field levels. We assume the local gap $\Delta \sim 25$ meV, since this yields a reasonable temperature scale below which the single-site entropy saturates to $\ln(2)$. This value of Δ is somewhat larger than the above quoted spin gap, seen using neutrons, near the (100) wave

vector, but we attribute this difference to the dispersion of the magnetic exciton.

While the measured magnetic susceptibility [49–51] for $T \lesssim 300$ K in these materials hints at a Curie-Weiss temperature scale ~ -150 K, we have shown that the true Θ_{CW} must be shifted by $\sim 0.1\Delta$ due to the local spin gap, so we estimate $\Theta_{\text{CW}} \sim -120$ K; dividing this by zJ^2, with the FCC coordination number $z = 12$ and moment size $J = 2$, we crudely estimate $\gamma_m \sim 0.25$ meV.

Next, to explain T^* for the Ising octupolar symmetry breaking, we must estimate the octupolar coupling constant in Eq. (8). We do not have any microscopic estimate for γ_2. Assuming $\gamma_2 \ll \Delta$, so this inte-site coupling is weaker than the on-site CEF splitting Δ, if we set $\gamma_2 \sim 5$ meV, we find the Ising ferro-octupolar exchange $6\gamma_m\gamma_2/\Delta \sim 7$ K. Using a classical FCC Ising model to describe the ferrooctupolar order, the known results for the Ising transition temperature [52], lead us to estimate an ordering temperature $T^* \sim 70$ K, somewhat larger than the experimental result. (We note that although we have explored the detailed consequences for $\gamma_2 > 0$, we are unable to rule out the possibility that $\gamma_2 < 0$, which would favor antiferro-octupolar order. In this case, a larger value of $|\gamma_2| \sim 50$ meV would be necessary to explain the octupolar ordering temperature T^*; however, it is not then clear why the $\tau_x\tau_x$ coupling in Eq. (9) would not cause a leading quadrupolar instability. Moreover, we do not have a microscopic explanation for such an antiferro-octupolar coupling.)

Turning to the measured exciton gap from inelastic neutron scattering, if we assume a Weiss field $\mathcal{B}_{\text{oct}} \sim 2.5$ meV (which is $\sim T^*/2$), then using the above Δ, γ_m, we find $\lambda(\mathbf{K}) \sim 25$ meV, larger than the measured exciton gap at $\mathbf{K}$. Choosing a larger $\gamma_m \sim 1$ meV leads to $\lambda(\mathbf{K}) \sim 14$ meV, in better agreement with the data. These uncertainties in γ_m might reflect the possibility that other magnetic exchange terms could be important, beyond a single isotropic Heisenberg coupling. Figure 3 shows the dynamical spin structure factor

$$\mathcal{S}(\mathbf{k}, \omega) \propto \sqrt{\frac{\mathcal{B}_{\text{oct}} + \Delta}{\mathcal{B}_{\text{oct}} + \Delta + 4\gamma_m\eta_{\mathbf{k}}}}\,\delta(\hbar\omega - \lambda(\mathbf{k})), \quad (25)$$

plotted after powder averaging, and including the Os^{6+} form factor. We find a high intensity gapped band in an energy window $\sim(0.5\Delta, \Delta)$, with the largest intensity concentrated at $k = \pi/a$, which corresponds to type-I ordering wave vector $\mathbf{K} = (\pi/a, 0, 0)$. We have assumed the Os-Os distance to be $a\sqrt{2}$, with $a = 4$ Å as the typical cubic lattice constant for such perovskite crystals.

We finally note that for a smaller gap Δ and stronger intersite exchange, the octupolar order can coexist with dipolar order or even be totally preempted by Bose condensation of the magnetic exciton. The resulting conventional type-I AFM state can have a small ordered moment if it is close to the exciton condensation transition. We propose this scenario for Sr_2MgOsO_6, which appears to have a smaller Δ (based on its entropy) and a larger γ_m (based on its Curie-Weiss temperature), and exhibits a type-I AFM ground state with an ordered moment $\sim 0.6\mu_B$, much smaller than the moment size $\sim 1.88\mu_B$ inferred from high temperature susceptibility measurements [53]. Weak tetragonal deformation in Sr_2MgOsO_6 will split the non-Kramers doublet and partially the triplet. In this case, the magnetic exciton condensation proposed here might still be of some relevance. However, we note that strong deformation may partially suppress the contribution of the orbital angular momentum, and drive the system closer to an orbitally quenched $S = 1$ magnet.

VIII. SUMMARY

We have presented arguments in this work in favor of octupolar ordering of $J = 2$ ions on the FCC lattice which is relevant to a family of complex $5d^2$ oxides, and identified a microscopic mechanism for generating ferro-octupolar

coupling. Further theoretical and experimental work, perhaps using magnetostriction as discussed in Ref. [16] or magnetic Raman scattering as explored here, is needed to provide smoking gun signatures of the ferro-octupolar symmetry breaking. For Raman scattering, our illustrative field scale $B = 0.04\,\Delta$ corresponds to ~ 10 Tesla. Such experiments may require single crystals of suitable sizes. It may also be useful to carry out more detailed microscopic calculations to compute the sign of the octupolar exchange; as noted above, the possibility of antiferro-octupolar order is not ruled out by our work. Another interesting experimental direction would be to apply pressure on the cubic DPs discussed here in an attempt to induce Bose condensation of the magnetic excitons. Our finding of a perturbative microscopic mechanism to induce octupolar couplings via excited crystal field levels through the combination of intersite orbital repulsion and Heisenberg spin exchange is general enough to be applicable to other lattice geometries. However, the specific competition between quadrupolar and octupolar orders will depend on details of the crystal structure. Finally, this mechanism we have identified may also be of potential importance in heavy fermion compounds, where underlying intersite orbital repulsion and spin exchange interactions needed to drive ferrooctupolar exchange can be induced via coupling to conduction electrons.

[1] P. Santini, S. Carretta, G. Amoretti, R. Caciuffo, N. Magnani, and G. H. Lander, Rev. Mod. Phys. **81**, 807 (2009).

[2] K. Haule and G. Kotliar, Nat. Phys. **5**, 796 (2009).

[3] H.-H. Kung, R. E. Baumbach, E. D. Bauer, V. K. Thorsmølle, W.-L. Zhang, K. Haule, J. A. Mydosh, and G. Blumberg, Science **347**, 1339 (2015).

[4] H.-H. Kung, S. Ran, N. Kanchanavatee, V. Krapivin, A. Lee, J. A. Mydosh, K. Haule, M. B. Maple, and G. Blumberg, Phys. Rev. Lett. **117**, 227601 (2016).

[5] P. Santini and G. Amoretti, Phys. Rev. Lett. **85**, 2188 (2000).

[6] J. A. Paixão, C. Detlefs, M. J. Longfield, R. Caciuffo, P. Santini, N. Bernhoeft, J. Rebizant, and G. H. Lander, Phys. Rev. Lett. **89**, 187202 (2002).

[7] A. Kiss and P. Fazekas, Phys. Rev. B **68**, 174425 (2003).

[8] Y. Tokunaga, D. Aoki, Y. Homma, S. Kambe, H. Sakai, S. Ikeda, T. Fujimoto, R. E. Walstedt, H. Yasuoka, E. Yamamoto, A. Nakamura, and Y. Shiokawa, Phys. Rev. Lett. **97**, 257601 (2006).

[9] T.-h. Arima, J. Phys. Soc. Jpn. **82**, 013705 (2013).

[10] A. Sakai and S. Nakatsuji, J. Phys. Soc. Jpn. **80**, 063701 (2011).

[11] T. J. Sato, S. Ibuka, Y. Nambu, T. Yamazaki, T. Hong, A. Sakai, and S. Nakatsuji, Phys. Rev. B **86**, 184419 (2012).

[12] M. Tsujimoto, Y. Matsumoto, T. Tomita, A. Sakai, and S. Nakatsuji, Phys. Rev. Lett. **113**, 267001 (2014).

[13] K. Hattori and H. Tsunetsugu, J. Phys. Soc. Jpn. **85**, 094001 (2016).

[14] F. Freyer, J. Attig, S. B. Lee, A. Paramekanti, S. Trebst, and Y. B. Kim, Phys. Rev. B **97**, 115111 (2018).

[15] S. B. Lee, S. Trebst, Y. B. Kim, and A. Paramekanti, Phys. Rev. B **98**, 134447 (2018).

[16] A. S. Patri, A. Sakai, S. B. Lee, A. Paramekanti, S. Nakatsuji, and Y. B. Kim, Nat. Commun. **10**, 4092 (2019).

[17] L. Fu, Phys. Rev. Lett. **115**, 026401 (2015).

[18] J. W. Harter, Z. Y. Zhao, J.-Q. Yan, D. G. Mandrus, and D. Hsieh, Science **356**, 295 (2017).

[19] S. Hayami, H. Kusunose, and Y. Motome, Phys. Rev. B **97**, 024414 (2018).

[20] B. J. Kim, H. Jin, S. J. Moon, J.-Y. Kim, B.-G. Park, C. S. Leem, J. Yu, T. W. Noh, C. Kim, S.-J. Oh, J.-H. Park, V. Durairaj, G. Cao, and E. Rotenberg, Phys. Rev. Lett. **101**, 076402 (2008).

[21] K. W. Plumb, J. P. Clancy, L. J. Sandilands, V. V. Shankar, Y. F. Hu, K. S. Burch, H.-Y. Kee, and Y.-J. Kim, Phys. Rev. B **90**, 041112(R) (2014).

[22] A. A. Aczel, J. P. Clancy, Q. Chen, H. D. Zhou, D. Reig-i-Plessis, G. J. MacDougall, J. P. C. Ruff, M. H. Upton, Z. Islam, T. J. Williams, S. Calder, and J.-Q. Yan, Phys. Rev. B **99**, 134417 (2019).

[23] A. Revelli, C. C. Loo, D. Kiese, P. Becker, T. Fröhlich, T. Lorenz, M. Moretti Sala, G. Monaco, F. L. Buessen, J. Attig,

M. Hermanns, S. V. Streltsov, D. I. Khomskii, J. van den Brink, M. Braden, P. H. M. van Loosdrecht, S. Trebst, A. Paramekanti, and M. Grüninger, Phys. Rev. B **100**, 085139 (2019).

[24] G. Khaliullin, Phys. Rev. Lett. **111**, 197201 (2013).

[25] T. Dey, A. Maljuk, D. V. Efremov, O. Kataeva, S. Gass, C. G. F. Blum, F. Steckel, D. Gruner, T. Ritschel, A. U. B. Wolter, J. Geck, C. Hess, K. Koepernik, J. van den Brink, S. Wurmehl, and B. Büchner, Phys. Rev. B **93**, 014434 (2016).

[26] K. Pajskr, P. Novák, V. Pokorný, J. Kolorenč, R. Arita, and J. Kuneš, Phys. Rev. B **93**, 035129 (2016).

[27] Q. Chen, C. Svoboda, Q. Zheng, B. C. Sales, D. G. Mandrus, H. D. Zhou, J.-S. Zhou, D. McComb, M. Randeria, N. Trivedi, and J.-Q. Yan, Phys. Rev. B **96**, 144423 (2017).

[28] A. Paramekanti, D. J. Singh, B. Yuan, D. Casa, A. Said, Y.-J. Kim, and A. D. Christianson, Phys. Rev. B **97**, 235119 (2018).

[29] C. Svoboda, M. Randeria, and N. Trivedi, Phys. Rev. B **95**, 014409 (2017).

[30] A. E. Taylor, S. Calder, R. Morrow, H. L. Feng, M. H. Upton, M. D. Lumsden, K. Yamaura, P. M. Woodward, and A. D. Christianson, Phys. Rev. Lett. **118**, 207202 (2017).

[31] A. E. Taylor, R. Morrow, M. D. Lumsden, S. Calder, M. H. Upton, A. I. Kolesnikov, M. B. Stone, R. S. Fishman, A. Paramekanti, P. M. Woodward, and A. D. Christianson, Phys. Rev. B **98**, 214422 (2018).

[32] D. D. Maharaj, G. Sala, C. A. Marjerrison, M. B. Stone, J. E. Greedan, and B. D. Gaulin, Phys. Rev. B **98**, 104434 (2018).

[33] G. Chen, R. Pereira, and L. Balents, Phys. Rev. B **82**, 174440 (2010).

[34] G. Chen and L. Balents, Phys. Rev. B **84**, 094420 (2011).

[35] C. Svoboda, M. Randeria, and N. Trivedi, arXiv:1702.03199.

[36] J. Romhányi, L. Balents, and G. Jackeli, Phys. Rev. Lett. **118**, 217202 (2017).

[37] L. Lu, M. Song, W. Liu, A. P. Reyes, P. Kuhns, H. O. Lee, I. R. Fisher, and V. F. Mitrović, Nat. Commun. **8**, 14407 (2017).

[38] W. Liu, R. Cong, E. Garcia, A. P. Reyes, H. O. Lee, I. R. Fisher, and V. F. Mitrović, Physica B **536**, 863 (2018).

[39] D. Hirai and Z. Hiroi, J. Phys. Soc. Jpn. **88**, 064712 (2019).

[40] D. D. Maharaj, G. Sala, M. B. Stone, E. Kermarrec, C. Ritter, F. Fauth, C. A. Marjerrison, J. E. Greedan, A. Paramekanti, and B. D. Gaulin, Phys. Rev. Lett. **124**, 087206 (2020).

[41] K. Kubo and T. Hotta, Phys. Rev. B **95**, 054425 (2017).

[42] T. P. Devereaux and R. Hackl, Rev. Mod. Phys. **79**, 175 (2007).

[43] M. Ye, H.-H. Kung, P. F. S. Rosa, E. D. Bauer, Z. Fisk, and G. Blumberg, Phys. Rev. Mater. **3**, 065003 (2019).

[44] B. S. Shastry and B. I. Shraiman, Phys. Rev. Lett. **65**, 1068 (1990).

[45] The work by Shastry and Shraiman [44] focused on resonant Raman scattering for the two-photon Raman process to sense the three-site spin chirality.

[46] S. Sachdev and R. N. Bhatt, Phys. Rev. B **41**, 9323 (1990).

[47] F.-Y. Li and G. Chen, Phys. Rev. B **100**, 045103 (2019).

[48] S. Das, D. Nafday, T. Saha-Dasgupta, and A. Paramekanti, Phys. Rev. B **100**, 140408 (2019).

[49] C. M. Thompson, J. P. Carlo, R. Flacau, T. Aharen, I. A. Leahy, J. R. Pollichemi, T. J. S. Munsie, T. Medina, G. M. Luke, J. Munevar, S. Cheung, T. Goko, Y. J. Uemura, and J. E. Greedan, J. Phys.: Condens. Matter **26**, 306003 (2014).

[50] E. Kermarrec, C. A. Marjerrison, C. M. Thompson, D. D. Maharaj, K. Levin, S. Kroeker, G. E. Granroth, R. Flacau, Z. Yamani, J. E. Greedan, and B. D. Gaulin, Phys. Rev. B **91**, 075133 (2015).

[51] C. A. Marjerrison, C. M. Thompson, A. Z. Sharma, A. M. Hallas, M. N. Wilson, T. J. S. Munsie, R. Flacau, C. R. Wiebe, B. D. Gaulin, G. M. Luke, and J. E. Greedan, Phys. Rev. B **94**, 134429 (2016).

[52] J. W. Essam and M. E. Fisher, J. Chem. Phys. **38**, 802 (1963).

[53] R. Morrow, A. E. Taylor, D. J. Singh, J. Xiong, S. Rodan, A. U. B. Wolter, S. Wurmehl, B. Büchner, M. B. Stone, A. I. Kolesnikov, A. A. Aczel, A. D. Christianson, and P. M. Woodward, Sci. Rep. **6**, 32462 (2016).